Hindawi
Journal of Advanced Transportation
Volume 2018, Article ID 6752574, 17 pages
https://doi.org/10.1155/2018/6752574

Research Article

Speed Behavior of Passenger Car on Helical Ramps and Helical Bridges in Mountain Riverside City

Jin Xu,[1] **Jinghou Fu**,[2] **Xiaoming Liu**,[2] **and Yiming Shao**[3]

[1]*Professor, Chongqing Key Laboratory of "Human – Vehicle -Road" Cooperation & Safety for Mountain Complex Environment, Chongqing Jiaotong University, No. 66, Xuefu Ave., Chongqing 400074, China*
[2]*Postgraduate Student, College of Traffic and Transportation, Chongqing Jiaotong University, No. 66, Xuefu Ave., Chongqing 400074, China*
[3]*Professor, College of Traffic and Transportation, Chongqing Jiaotong University, No. 66, Xuefu Ave., Chongqing 400074, China*

Correspondence should be addressed to Jin Xu; yhnl272727@163.com

Received 6 June 2018; Accepted 31 October 2018; Published 13 November 2018

Academic Editor: Md. Mazharul Haque

Copyright © 2018 Jin Xu et al. This is an open access article distributed under the Creative Commons Attribution License, which permits unrestricted use, distribution, and reproduction in any medium, provided the original work is properly cited.

Helix alignment can allow for a rapid change in road elevation in size-constrained spaces, and it is becoming increasingly popular in interchange design throughout the world. However, driving patterns and vehicle operating characteristics have not been clearly defined on helical ramps. This work conducted field driving tests on four helical ramps located in Chongqing, China. The trajectory, speed, and acceleration of vehicles under normal driving conditions were collected. Thus speed characteristics and speed patterns on helical ramps, as well as their affecting factors, were obtained and analyzed. The findings in this study can provide basic data referencing for designers and engineers, to help them understand how a multilayered helical ramp works, thus to essentially improve the safety level of helix ramps. Moreover, our findings allow bridge designers to understand whether the actual vehicle operating conditions acted in accordance with their expected design requirements, i.e., whether the expected design requirements are achieved.

1. Introduction

Helix curves are effective for overcoming elevation differences in size-constrained spaces and for allowing the route to ascend rapidly [1]. A helical ramp is the most effective design for achieving traffic transition in areas with highly limited space and large differences in elevation. Therefore, in recent years, helix curves are being used more extensively in highway and municipal engineering projects, such as expressways, tunnels, interchanges, and urban roads. Moreover, as the number of cities and towns in mountainous areas increases and the land use in cities intensifies, the use of helical ramps and helical bridges will become more extensive. In addition, the increasing navigational clearance requirements for river-spanning bridges, along with increasing environmental protection awareness, also promote the use of helical ramps. In China Shanghai Nanpu Bridge is a famous site where helical ramps are used in the interchange at cross-river bridge, as shown in Figure 1(a). Chongqing is a large and flourishing mountain city and is famous for its numerous complex bridges and roadways, the helical bridge in Figure 1(b) is a ramp of Chongqing Sujiaba Interchange, and the helical bridge in Figure 1(c) is a segment of Hongyun Road, which is under construction and is to be opened to traffic in Apr. 2019. The helical ramp in Figure 1(d) is an emergency lane linked to Tianxingzhou Yangtze River Bridge, located in Wuhan, China. Similarly, in other countries out of China helical bridges also were adopted in mountain roads and interchanges; for instance, Nanadaru Bridge Loop in Figure 1(e) is a helical bridge constructed in Kawazu, Japan, and Tokyo Rainbow Bridge Loop in Figure 1(f) is another helical bridge in Japan.

Compared to conventional ramps with general configurations, helical ramps and bridges have the following distinctive features:

(i) Lane keeping and steering control may have particular maneuvering demands for a driver when driving on a long, curvature-fixed helix curve.

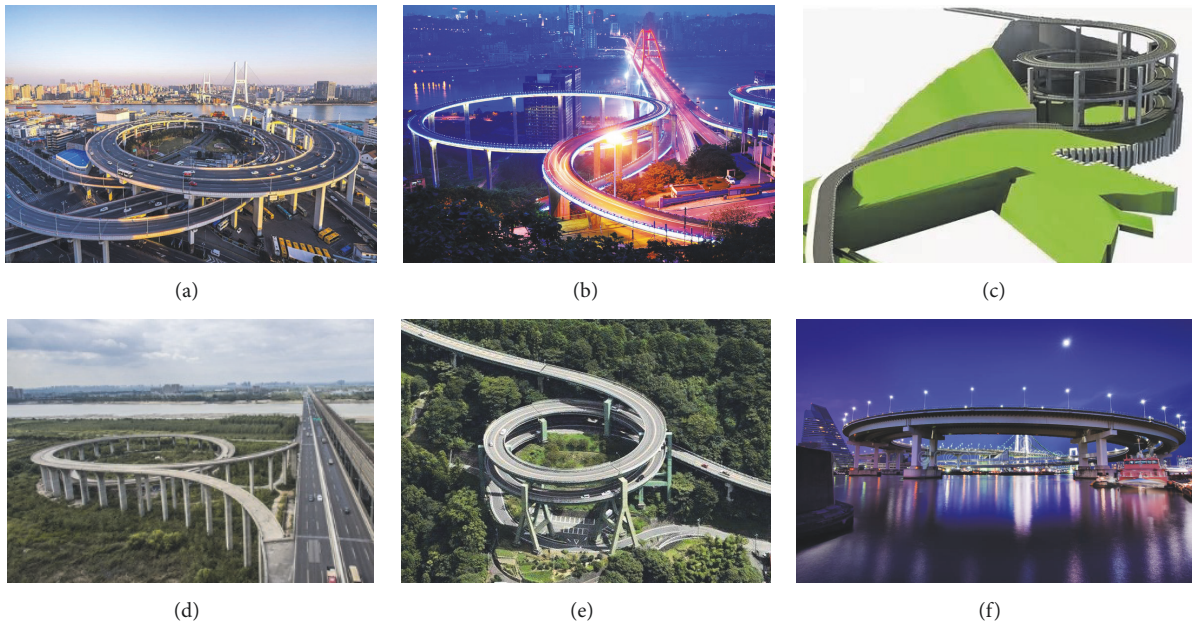

(a) (b) (c)

(d) (e) (f)

Figure 1: Helical bridges and helical ramps in and out of China. (a) Shanghai Nanpu Bridge, China; (b) Chongqing Sujiaba Interchange, China; (c) helical bridge of Hongyun Road in Chongqing, China; (d) helical emergency ramp of Tianxingzhou Yangtze River Bridge, China; (e) Nanadaru Bridge Loop, Japan; (f) Tokyo Rainbow Bridge Loop, Japan.

(ii) A one-directional steep slope (single gradient), meaning that an ascending ramp has a continuously increasing elevation and a descending ramp has a continuously decreasing elevation.

(iii) Large turning-angle loops with a curve angle exceeding 720° (currently, all helical ramps have two or more layers) and a continually changing vehicle direction while driving. In contrast, hairpin curves on a curvy mountainous road have a deflection angle of approximately 180°, and the loop ramps of a cloverleaf interchange, which are generally considered difficult to navigate, have angles of only approximately 270°.

Therefore, because of the distinctive alignment characteristics and driving conditions of helical ramps, there is an urgent need to investigate several related issues, such as whether the driving behavior and vehicle operating modes have any particularities, whether the driving behavior matchs the design expectations and driving assumptions, and, if any deviations exist, whether the extent of the deviation is serious. It is obvious that these issues are also the basis for improving the intrinsic safety of helical ramps at the design stage.

2. Literature Review

At present, relevant studies closely related to helical ramps mainly focus on the structural design of the ramp itself, such as the pier and beam layout [2], consolidation methods [3], structural force calculations [4, 5], and the treatment of foundations [6] and rarely focus on the driving behavior and vehicle operating performance within the helical ramps.

Existing studies are mainly devoted to investigating the vehicle operation/driving characteristics on conventional interchange ramps with general configurations. Among them, based on data obtained from a vehicle mounted GPS, Zhang et al. [7] established an operating speed model for interchange ramps as a function of curvature change rate and superelevation. Zhang et al. [8] used a radar speed gun to measure the speed of passenger cars in a deceleration lane and established an operating speed model at the theoretical gore and physical gore. Using a similar approach, Wang and Yang [9] measured the velocities of passenger cars at the theoretical gore, the mid-point of the deceleration lane, and the physical gore of an expressway interchange and obtained a model for calculating the lengths of the deceleration lanes. Guo et al. [10] used a driving simulator to simulate the driving process on the entrance and exit ramps of expressways and analyzed speed behavior in the deceleration and acceleration lanes based on the use of the accelerator/brake pedals. Wang et al. [11] used vehicle-mounted equipment to continuously measure driver eye movement, vehicle speed, and lane usage in the expressway interchange area and analyzed the driving behavior in a merging area, ramp area, and diverging area.

Polus et al. [12] used aerial cameras to record the continuous driving behavior of a vehicle in a freeway interchange merging area and obtained the merging point of vehicles exiting from the acceleration lane (entering the mainline traffic flow), as well as their continuous speed and acceleration. Using similar methods, they also investigated the driving behavior in the diverging area and determined the exact location and spatial distribution of the vehicles exiting the mainline traffic flow (entering the deceleration lane) [13], as well as their deceleration rates. These two works provided valuable data support for distinguishing the design parameters for parallel and tapered deceleration/acceleration lanes. Ahammed et al. [14] used a radar gun to track the speed of vehicles traveling in the merging area of an interchange and developed the model of operating speed, acceleration,

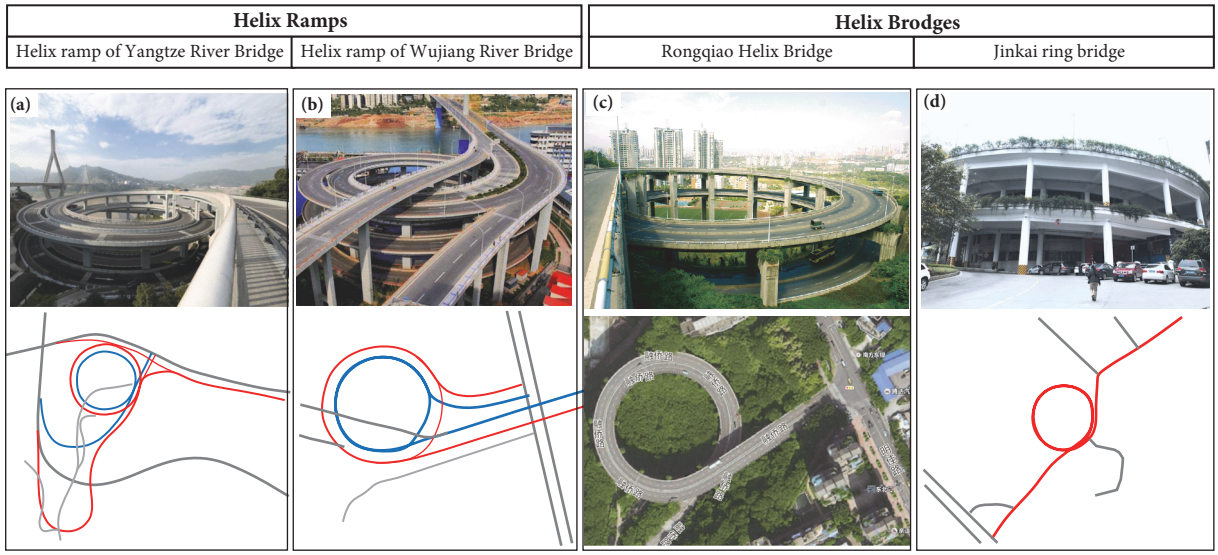

Figure 2: Helical ramps and helical bridges selected in this study.

and distance of the acceleration lane. Fitzpatrick et al. [15] analyzed the rationality of the basic assumptions for vehicle deceleration in the merging areas and the applicability of the deceleration rate in current design standards in U.S. Taking roundabouts as the research object, Zirkel et al. [16] discussed the effect of 85th percentile speed distribution and sight distance of the drivers on crash rates for low-volume single-lane roundabouts. Perco et al. [17] established an operating speed model for the merging area and diverging area of two types of interchanges by using the data obtained from radar guns. Yang [18] investigated the acceleration characteristics for metered on-ramps with various geometric features and also figured out speed profiles to guide the design of acceleration-lane length, using automatic video processors. Li and Sun [19] collected merging maneuvers of 370 drivers from the NGSIM (Next Generation Simulation Program) dataset and developed a novel data mining tool, called two-step cluster analysis, and the merging maneuver was divided into four clusters by this tool. Lvu et al. [20] analyzed the effect of driver's gender, occupation, and experience on behavior while driving on a freeway deceleration lane based on field operational test data. However, all the above studies concentrate on merging/diverging traffic and deceleration/acceleration areas and do not concentrate on the ramps.

In summary, at present, there are no reports available on driving behavior on helical ramps or helical bridges. Thus, researchers, designers, and managers are not able to understand the operating characteristics of vehicles traveling on helical ramps (bridges). Among driving behavior parameters, speed is a basic response of vehicle operation and driver behavior; at the same time, it is the core parameter that controls the interchange geometry and configuration in design. For this reason, a natural driving test involving passenger cars traveling on helical ramps was carried out in this study. Operating parameters were collected continuously using on-board equipment, and the speed amplitude and change patterns of a passenger car on a helical ramp (bridge) were determined. The findings of this study answered the following questions:

(i) How does vehicle speed change when a car is driving on a helical ramp? Will the continually decreasing or increasing elevation of the helical ramp cause a change in driving speed?

(ii) What kind of speed changes occur at the two ends of the helical ramp?

(iii) Do there exist diversified patterns in speed change along a helical ramp for individuals?

(iv) Are the speed amplitude consistent with the design expectations of the helical ramp, and do any serious deviations exist?

3. Experiment Design

In view of the structural form and geometric feature of helical ramps, vehicles with on-board apparatuses were used to conduct field driving test in this study. The operational parameters and the steering input of the driver were collected continuously while the car was traveling on the helical ramp and helical bridge. The following section provides a detailed description of the experimental design.

3.1. Experimental Objects. Four sites within the jurisdiction of Chongqing, China, were selected: the Rongqiao Helix Bridge, which is located in an urban area of Chongqing City, and the Wujiang Bridge helix ramp, Yangtze River Bridge helix ramp, and Jinkai ring bridge, which are located in the Fuling District, a city approximately 130 km from Chongqing. The Jinkai ring bridge loops around the Jinkai Ornamental Shopping Mall in two loops; that is, the building is encircled by the helix bridge. Table 1 lists the main technical parameters of the four experimental objects, and Figure 2 shows a panoramic view of the two helical ramps and two helical bridges, and their surrounding road network.

Table 1: Main technical parameters of the test objects.

Test object name	Location	V_d (km/h)	Traffic lane number	Travel direction	Structural form	G (%)	Horizontal Radius (m)	Number of layers	Test vehicles	Participant identification number
Yangtze River Bridge (YZ)	Fuling District, Chongqing	20	1	one-way	Single column pier	4.5%	39.525 m for ascending ramp, 50 m for descending ramp	2	Buick GL8 Firstland, Buick Buddha	D6–D15
Wujiang Bridge (WJ)	Fuling District, Chongqing	30	2	one-way	Single pier continuous cantilever beam	4.5%	51 m for ascending ramp, 38.25 m for descending ramp	2	Buick GL8 Firstland, Buick Buddha	D6–D13
Rongqiao Helix Bridge (RQ)	Urban area of Chongqing	40	2	one-way	Door-type multi-span continuous beam	6%	Median strip radius 55 m	2	Benz Vito, Toyota Hiace, Buick Buddha	D1–D5; D10–D11; D13–D15
Jinkai Ring Bridge (JK)	Fuling District, Chongqing	20	2	two-way	Door-type multi-span continuous beam	5–6%	30 m (centerline)	2	Buick Buddha	D8–D15

V_d: design speed; G: gradient of the ramp.

(a) (b)

Figure 3: On-board equipment used in naturalistic data collection. (a) The composition of AHRS, fixed on the test car; (b) Laser Doppler Tachometer.

The pavement of the experimental objects was clean, smooth, and labelled with clear and complete markings. Field driving tests were carried out from 10:00 am to 17:30 pm to avoid peak traffic times in the morning and evening, and the drivers steered their cars in free flow traffic in all test rounds (occasionally, the subject car was obstructed by slow-moving forward vehicles, such as trucks). The driving tests were conducted from March 2016 to October 2017.

3.2. Testing Equipment and Vehicles. Radar gun and GPS are the two most commonly used methods for obtaining vehicle speed. The former measures the vehicle speed at a particular location. This method has limitations because the angle between direction of travel and the longitudinal axis of the gun cannot exceed 10–30°, the observation distance cannot exceed 400 m, and there are also minimum speed requirements. Therefore, radar guns are only suitable for measuring speed in the merging and diverging areas of interchanges and cannot be used for continuous speed acquisition on large-angle ramps. GPS is mainly used for recording the continuous speed of a single vehicle. However, as the vehicle travels on a helical ramp, the upper layer decks significantly obstruct the GPS signal, causing a disruption in the real-time positioning data and a gap in the recorded speed data.

In this study, we recorded the vehicle trajectory and speed using two types of apparatuses. One is an Attitude and Heading Reference System (AHRS), which consisted of an inertial measurement unit (IMU, an integration of triple-direction accelerometer and gyroscope) combined with a dual GPS antenna, as illustrated in Figure 3(a). When the GPS signal was lost, the algorithm integrated the acceleration signal measured by the IMU to obtain the vehicle position and performed an offline data compensation. The other is a Laser Doppler Tachometer, as shown in Figure 3(b). The speed results from the ARHS measured on the tangent section were used for calibrating the Laser Doppler Tachometer, and the speed data output from the latter was used in the analysis. In addition, cameras were fixed to the front and rear windows to record the environment in front of and behind the vehicle, and videos were used in postprocessing to analyze the reasons for fluctuations in the speed. We rented seven-seat commercial vehicles as the test vehicles, which included a Buick Buddha, Buick GL8 Firstland, Benz Vito, and Toyota Hiace, of which the first three are MPVs and the last is minivan. The distribution of these vehicles on the four sites is listed in Table 1.

3.3. Participants (Drivers). A total of 15 healthy drivers participated in our field driving test. The age range of the participants was 23–57 years, with an average age of 38. Seven drivers were 20–26 years old, three drivers were 35–39 years old, three drivers 40-49 years old, and two drivers were 55–59 years old. The length of their driving experience ranged from 1 to 31 years, averaging 10 years overall. Eight participants had 1–4 years of experience, two had 5–9 years, two had 15–19 years, two had 20–24 years, and one had 30–34 years. The subjects were recruited from an urban area of Chongqing and were familiar with the vehicle model used in this study. Before the test, the participants were instructed to drive the vehicles according to their daily driving style and habits; no requirements were imposed and no suggestions were given regarding the driving process. If a participant inquired about any requirements or speed control limits before or during the driving test, the given answer was "no requirements." This condition was intended to preserve the natural driving habits of the participants to the greatest extent possible.

3.4. Procedure of Driving Test. The route for each trial site was arranged before the field test was conducted, including the location where the personnel started to record and save the data from onboard instruments and the location where the driver turned his/her car after driving off the helical ramp. For example, the helical ramp on the Fuling Yangtze River Bridge is presented in Figure 4 to illustrate the path

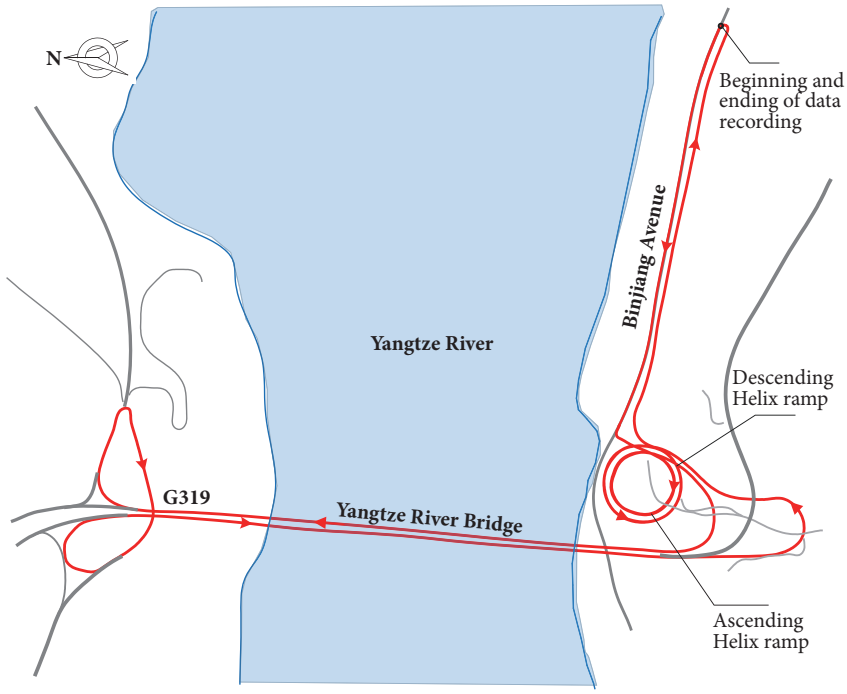

Figure 4: Route of field driving test for helical ramp of Fuling Yangtze River Bridge.

of the vehicle in one loop of the driving test. At each site, before we began recording data, the system time of each instrument was calibrated with the host computer. After each subject completed his/her required driving round, the on-board apparatus stopped recording.

For each test object, we designated one course on the ascending ramp and one course on the descending ramp as a complete round. We requested each driver to complete 4–6 rounds. The purpose was to ascertain whether the first lap experience was significantly different from the subsequent laps. At the same time, it also ensured an adequate number of data samples and prevented a situation in which valid data could not be collected due to unforeseen circumstances occurring during a single round.

For each participant, we first segmented the continuous speed profile measured from a driver based on videos recorded by the front camera, one speed profile for one round, and secondly cut the speed data within the area of helical ramp and separate it from the original data, to ensure each ramp travel (ascending or downward) corresponding to one speed curve. Finally, the fluctuations and changing trends of the speed along the ramp were analyzed.

4. Overall Speed Characteristics on Helical Ramps (Bridges)

Design speed is the key parameter that controls the appearance, floor space, and operating performance of an interchange. In this section, we examine the coordination between the design of the helical ramp and the actual driving requirements based on the measured speed and analyze the speed behavior at two ends of the ramps.

4.1. Ascending Helical Ramps

4.1.1. General Characteristics. Figure 5 shows the continuous speed profiles within the range of the helix for each of the four test objects. Figure 5(a) presents the speed profiles of ten participants from the ascending ramp of the Fuling Yangtze River Bridge. When entering the ascending ramp from Binjiang Avenue, the driver had to wait at a traffic signal before making a 90° left turn onto the ramp, as shown in Figure 4. Therefore, the vehicles started from a very low speed and accelerated onto the helical ramp; i.e., there was an "initial acceleration" stage, i.e., Stage I, for approximately 60–90 m. Stage II, the main part of speed profiles that cover the range of helix ramp, seems wholly to show a slight increase along the distance travelled.

Figure 5(b) shows the speed profiles of eight participants on the ascending helical ramp of the Fuling Wujiang Bridge. Before entering the helical ramp, participants had to drive on a 60-m tangent after waiting for the left turn signal light on the mainline, as shown in Figure 2(b). The speed change trend in stage II merits our attention. We can see that, after a relatively intense acceleration period, the participants basically maintained a stable speed.

Figures 5(c) and 5(d) are the speed profiles for the Chongqing Rongqiao Helix Bridge and the Jinkai Ring Bridge, respectively. These two ramps are part of the road sections and not connecting ramps between two different roads. Therefore, no route change is necessary. We can see from the two figures that even though the speed fluctuates within the helical bridge, the overall amplitude is stable for the most part. In Figure 5(c), the reduction at end of speed profiles (Stage III) is caused by the fact that the vehicle needed to stop and wait at a traffic signal before it could enter the

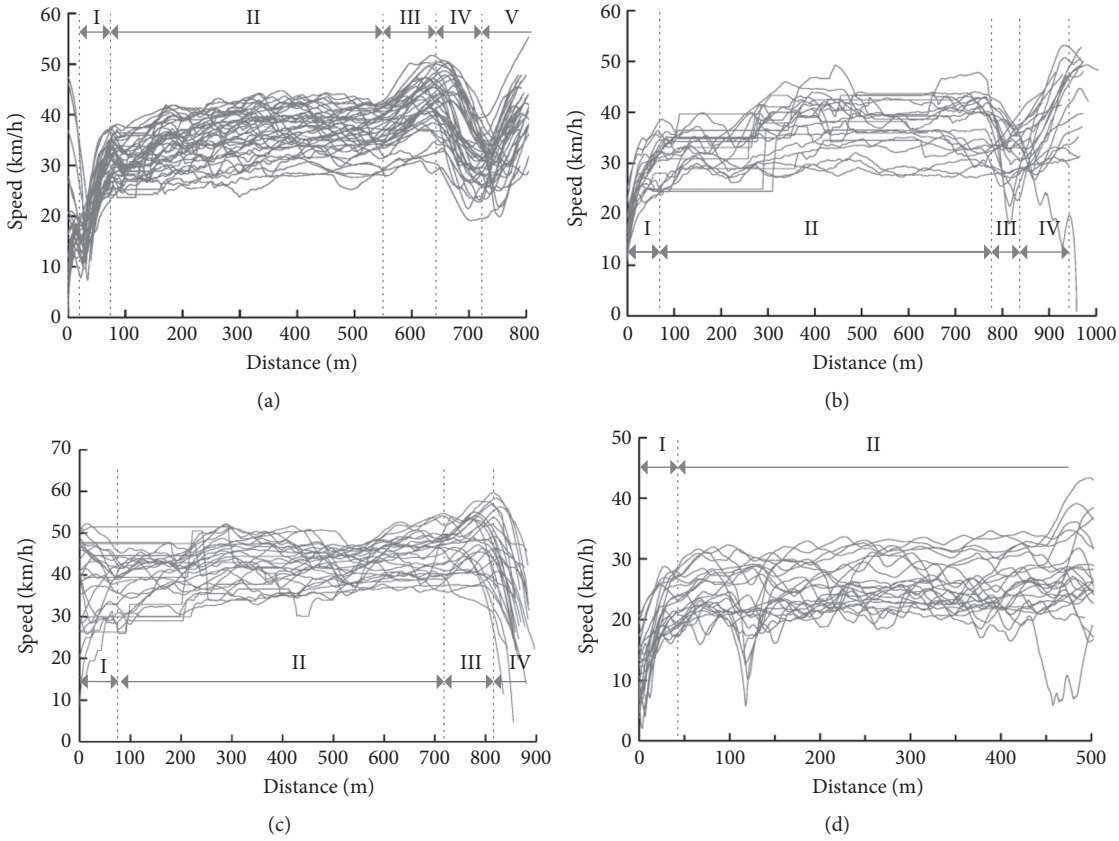

FIGURE 5: Driving speed on ascending ramp. (a) Ramp of Fuling Yangtze River Bridge, design speed (V_d) 20 km/h. (b) Ramp of Fuling Wujiang Bridge, V_d = 30 km/h. (c) Ramp of Chongqing Rongqiao Helix Bridge, V_d = 40 km/h. (d) Jinkai Ring Bridge, V_d = 20 km/h.

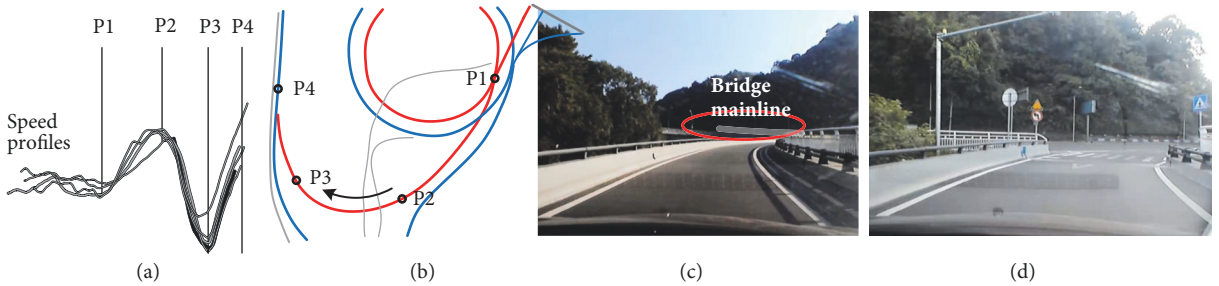

FIGURE 6: Feature points of speed change. (a) Driving speed; (b) feature points of speed change at merging area; (c)-(d) driver's line-of-sight environment corresponding to points P2 and P3.

intersected road, Jiaming Road. And in Figure 5(d) the speed profiles exhibit a slightly rising tendency along the distance travelled, which is similar to the speed change within Stage II in Figure 5(a).

After a comprehensive comparison of the measured speed of all participants, we can draw the following conclusions: First, the continuously increasing elevation did not cause any speed reduction for passenger cars; second, even though the design speed of the helical ramp of the Yangtze River Bridge was 20 km/h, the measured speed of most of participants ranged from 30 to 45 km/h. This indicates that the speed perception provided by the ramp environment to the driver is seriously inconsistent with the design expectations.

4.1.2. Feature Points. In Figure 5(a), while approaching the end of the ascending ramp, the speed curves for all participants show an initial increase (Stage III), followed by a rapid decrease (Stage IV), and finally another sharp increase (Stage V). Figures 6(a) and 6(b) show the feature points where the change in speed occurs, as well as their corresponding positions on the ramp. It is evident that the driver started to accelerate immediately after exiting the end point of the helix, P1. When arriving at P2, the mainline (bridge) and its traffic flow enter the sight line of the driver, as shown in Figure 6(c), causing the driver to decelerate subconsciously. When the speed experiences the lowest value at P3, shown in Figure 6(d), the driver begins to accelerate again. Location P4

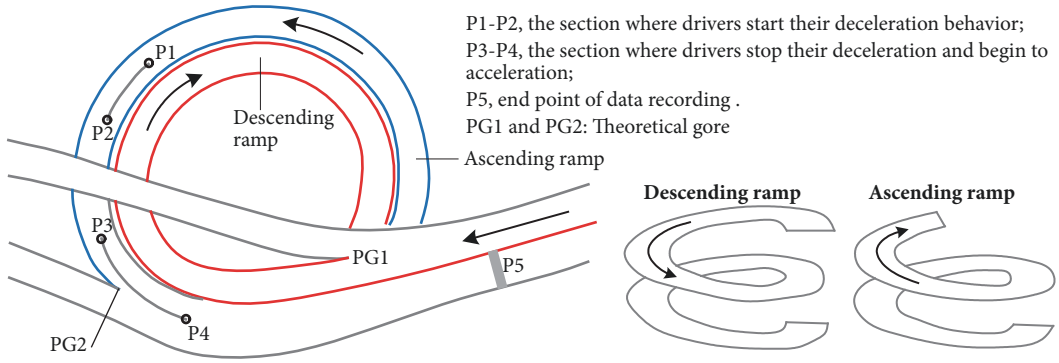

Figure 7: Feature points of speed change on the ascending ramp of Fuling Wujiang Bridge.

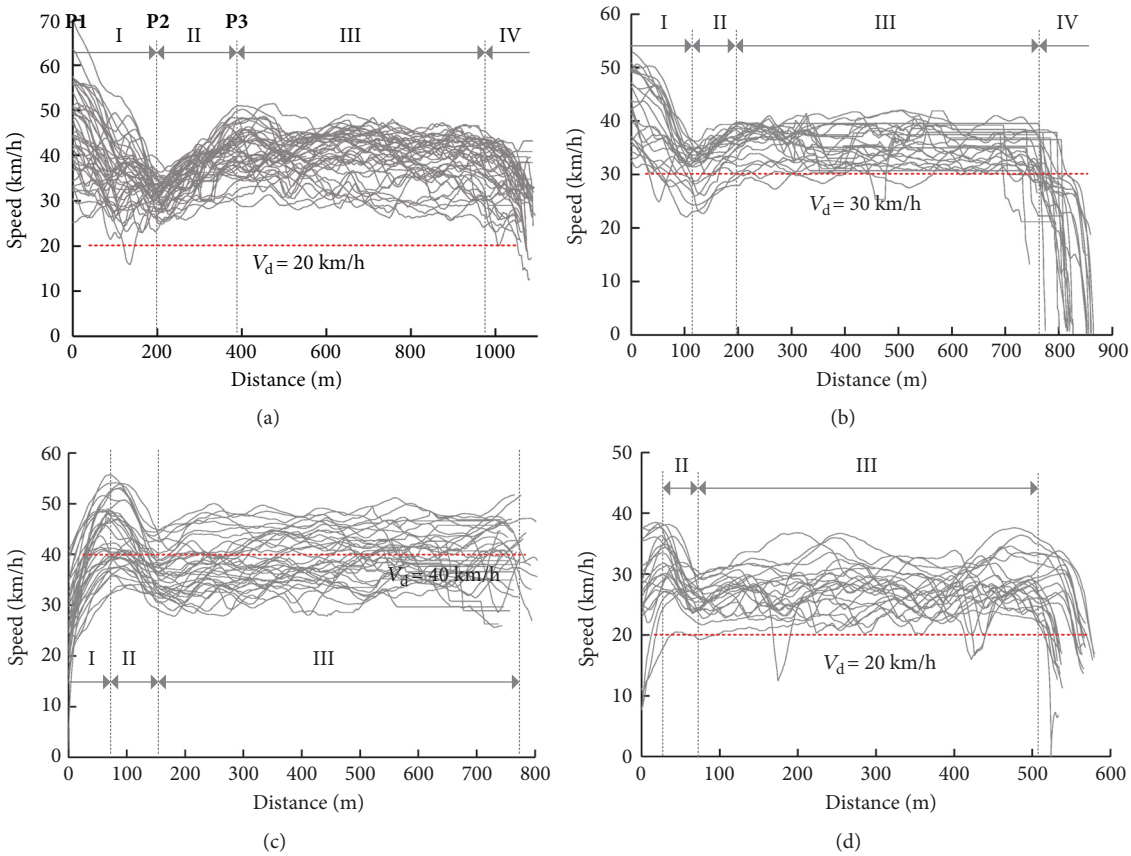

Figure 8: Driving speed on descending ramps. (a) Ramp of Fuling Yangtze River Bridge, design speed (V_d) 20 km/h. (b) Ramp of Fuling Wujiang Bridge, V_d = 30 km/h. (c) Ramp of Chongqing Rongqiao Helix Bridge, V_d = 40 km/h. (d) Jinkai Ring Bridge, V_d = 20 km/h.

is the end point of the taper, i.e., the theoretical gore, and also the end point for data recording.

Moreover, the speed profiles in Figure 5(b) show different levels of decreases in speed at the end of the ramp of Wujiang Bridge, i.e., Stage III. Based on the videos from the front camera and the diction of the driver, we suspected that the deceleration was caused by the driver observing the traffic conditions on the main bridge. The drivers began to accelerate again at the merge point, namely, Stage IV. The feature points of speed change along this ramp are present in Figure 7. Based on the above observations and the conditions observed on the end section of the helical ramp of Fuling Yangtze River Bridge, we conclude that the deceleration operation is a common driving behavior just before leaving the ramp.

4.2. Descending Helical Ramps

4.2.1. General Characteristics. Figure 8 shows the speed profiles for the four descending ramps. Figure 8(a) presents the speed on the ramp of Fuling Yangtze River Bridge. This ramp consists of two parts: part one is the curved ramp section

before the starting point of the helix and consists of three horizontal curves that account for 35% of the total ramp length; part two is the helical ramp section. It is evident from the figure that vehicle speed on the first part decreases significantly, starting from the theoretical gore. Therefore, the deceleration distance can be regarded as reflecting the natural habits of drivers. Moreover, the change in speed within the helical ramp range (Stage III) exhibited an overall descending trend in general.

Figure 8(b) shows the speed for the descending helical ramp of the Fuling Wujiang Bridge. The starting point of the speed profiles is located at the end of bridge mainline, and the end point is the position where the ramp meets Binjiang Avenue after reaching the ground level. Similarly, the speed curve trend shows a decrease first (Stage I), followed by an increase (Stage II), while remaining constant in the next section (Stage III). The decline of the speed curve in its end is caused by the fact that there is a traffic signal at the traffic merge point, so the vehicle should wait for the green signal before entering the mainline traffic flow.

Figure 8(c) shows the speed on the descending ramp of the Rongqiao Helix Bridge. Although the speed fluctuates slightly within the helical ramp (Stage III), it is obvious that the overall trend is constant. The intersection of Rongqiao Road and Mingjia Road is a T-junction; moreover, there is a pedestrian crossing at the beginning of the helical ramp (Figure 2(c)), so the vehicles need to decelerate or stop before accelerating onto Rongqiao Road. Therefore, the speeds in Figure 8(c) all begin with an acceleration until a peak value is reached, and then a deceleration is exhibited when entering the helical ramp. Finally, a constant speed is shown at the end. Figure 8(d) shows the speed on the descending ramp of the Jinkai Ring Bridge. The profiles show a similar trend to that of the Rongqiao Helix Bridge, except that the speed amplitude is slightly lower.

Based on Figure 8, we did not observe an increasing trend in speed when traveling on descending ramps, whether it was a helical ramp or a helical bridge, indicating that the continuously decreasing elevation along the distance did not result in an increase in the traveling speed of passenger cars.

4.2.2. Deceleration and Acceleration Length. From Figure 8(a) we can find that the deceleration distance (the distance between point P1 and point P2) of most participants is about 200 m. The feature points P1 to P3 on the ramp are marked in Figure 9, and we can see that the ending point of deceleration, P2, is just located on the middle of the hairpin curve, while the point P3, the ending point of followed acceleration, coincides with the start point of the helical ramp. Therefore, we may recognize the fact that drivers' deceleration and acceleration behavior in this case is highly depending on the geometric features of the ramp.

It is evident from Figure 8(b) that drivers decelerate when entering the ramp from the mainline (a 650 m long tangent) of Wujiang second bridge. We extracted the deceleration distance from the speed-distance curves for all participants at this location, and the results are shown in Figure 10(a). The distribution interval of the discrete points was 95–165 m,

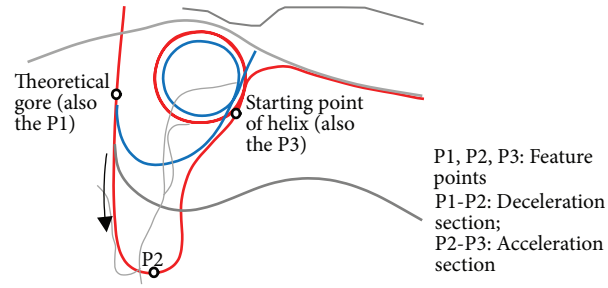

Figure 9: Feature points of speed change on the ascending ramp of Ramp of Fuling Yangtze River Bridge.

and the range of an average line was 110–129 m. Figure 10(b) shows the cumulative frequency of the deceleration distance, which obeys the Gamma distribution, shown in (1) and (2). The estimated values of parameters α and β are 65.778 (95CI: 39.01-111.92) and 1.841 (95CI: 1.09-3.11), respectively, and the 85th percentile deceleration distance is 138 m. The distribution of the end points of the deceleration distance was marked on this ramp, as shown in Figure 10(c), where L_{dmin} and L_{dmax} are the minimum and maximum deceleration distance, respectively. It is evident from the figure that the deceleration behavior lasts over the range of helical ramp, at approximately 1/3 of the circumference of the ramp.

$$f(x) = \frac{\alpha^{\beta}}{\Gamma(\alpha)} x^{\alpha-1} e^{-\beta x}, \quad x > 0 \tag{1}$$

$$\Gamma(\alpha) = \int_0^{+\infty} t^{x-1} e^{-t} \mathrm{d}t \tag{2}$$

Figure 11(a) shows the deceleration distances (the vehicle travelled in Stage II of Rongqiao Helical Bridge) of ten participants in an increasing order. The differences between different drivers are significant, with the average line ranging from 60 to 140 m. Figure 11(b) shows the cumulative frequency of the acceleration and deceleration distance, where parameters α and β of the Gamma distribution function for deceleration distance are estimated at 6.619 (95CI: 3.81-11.49) and 13.068 (95CI: 7.36-23.19), respectively. Figure 11(c) shows the feature points of the acceleration and deceleration behavior, where L1 and L2 are the minimum and maximum acceleration distance, respectively, while L4 marks the area within which the end points of driver deceleration behavior are distributed. Therefore, we can conclude that the deceleration will continue into the helical ramp range for a distance approximately 40% of the ramp circumference.

5. Speed Patterns on Helical Ramps (Bridges)

From the speed profiles set presented in Figures 5 and 8, we can get general understanding on speed change within the range of helical ramp, i.e., rising, falling, or stabilizing. However, for a specific participant, his/her speed preference might be the opposite of the overall trend in speed tendency; i.e., individual speed change might be masked and hide in the overall trend, while, for highway design and traffic safety, the

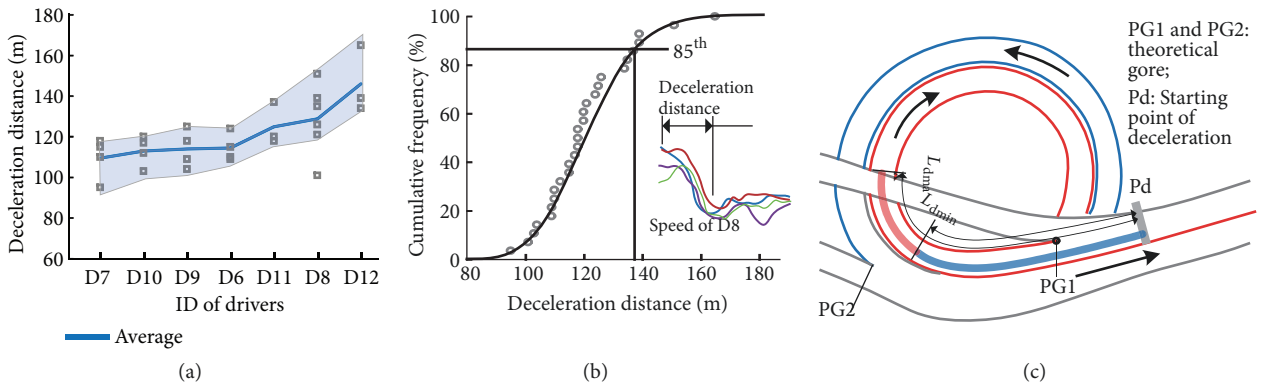

FIGURE 10: Deceleration distances on the descending ramp of Fuling Wujiang Bridge. (a) Deceleration distances of different test participants; (b) deceleration distance cumulative frequency curve; (c) deceleration distance distribution area.

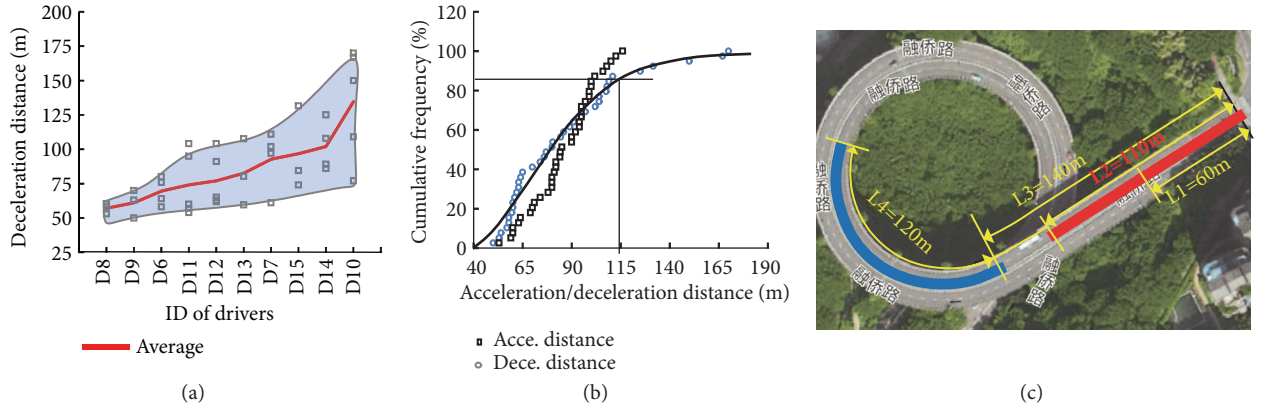

FIGURE 11: Deceleration distance on the descending ramp of the Rongqiao Helix Bridge. (a) Deceleration distances of different participants; (b) cumulative frequency curve of deceleration distance; (c) distribution area of deceleration distance.

behavior of individuals should be given equal weight to the behavior of average/overall level.

5.1. Method to Identify the Speed Patterns. Here we focus on the pattern of speed change within the range of helical ramp after drivers finish their initial acceleration and deceleration, i.e., changing patterns of speed curves of Stage II marked in Figure 5 and speed curves of Stage III marked in Figure 8. The gradient of speed, GV_1 and GV_2, was used to identify and define the speed pattern on a helical ramp, and GV_i was calculated by

$$GV_i = \frac{(V_{i+1} - V_i)}{(d_{i+1} - d_i)} \tag{3}$$

The method of getting GV_1 and GV_2 from a given speed profile was illustrated in Figure 12. Because the speed fluctuates locally along the distance, V_i was extracted from the trend line (fitting curve) of the measured data of speed. According to the shape of speed profiles in Figures 5 and 8, a broken line linked by three point can outline the trend and changing pattern of a given speed profile. Data point (GV_{1i}, GV_{2i}) would be determined and plotted in a plane coordinate after the valves of GV_1 and GV_2 were calculated.

In fact, the position of an arbitrary data point (GV_{1i}, GV_{2i}) in GV_1 —GV_2 coordinate is nothing more than subject to the following nine kinds, as shown in Figure 13, in which one situation corresponds to one speed pattern, i.e., the speed in the graph below the GV_1 —GV_2 coordinate. Therefore, we can recognize the speed pattern by using the data points (GV_{1i}, GV_{2i}).

5.2. Results of Speed Pattern Identifying. Using the method illustrated in Figure 12, data points (GV_{1i}, GV_{2i}) of all four ascending helical ramps and four descending ramps were obtained and displayed in the GV_1 —GV_2 coordinate, as shown in Figure 14. Comparing the quadrant distribution of (GV_{1i}, GV_{2i}) of ascending ramp against that of descending ramp, we find that there exists significant difference between speed patterns of ascending ramp and descending ramp. Taking YZ as example, for ascending ramp, twenty-seven data points are located in the first quadrant, and seventeen points are located in the fourth quadrant, while for descending ramp, of all forty-five points, twenty-one were in the fourth quadrant, and the rest were scattered in other three quadrants. The quadrant distribution of WJ' ascending ramp is similar to that of YZ' ascending ramp; i.e., patterns I, IV,

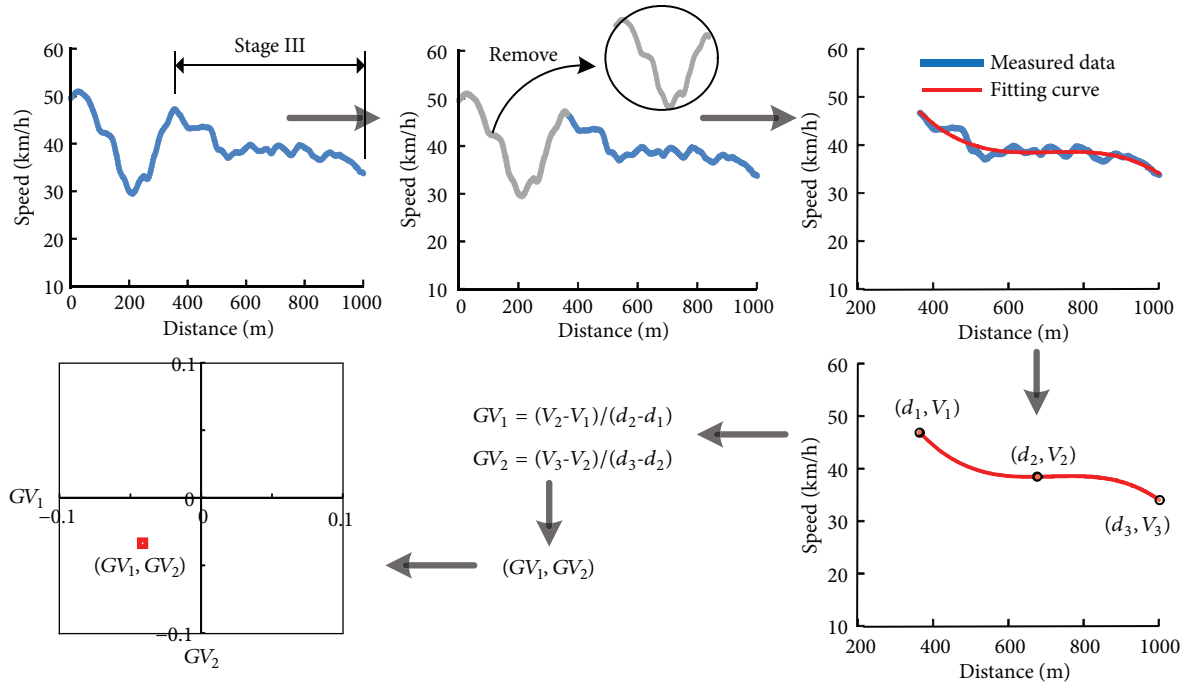

FIGURE 12: Method to get the value of GV_1 and GV_2 from a measured speed profile and show the point of (GV_1, GV_2) in a plane coordinate.

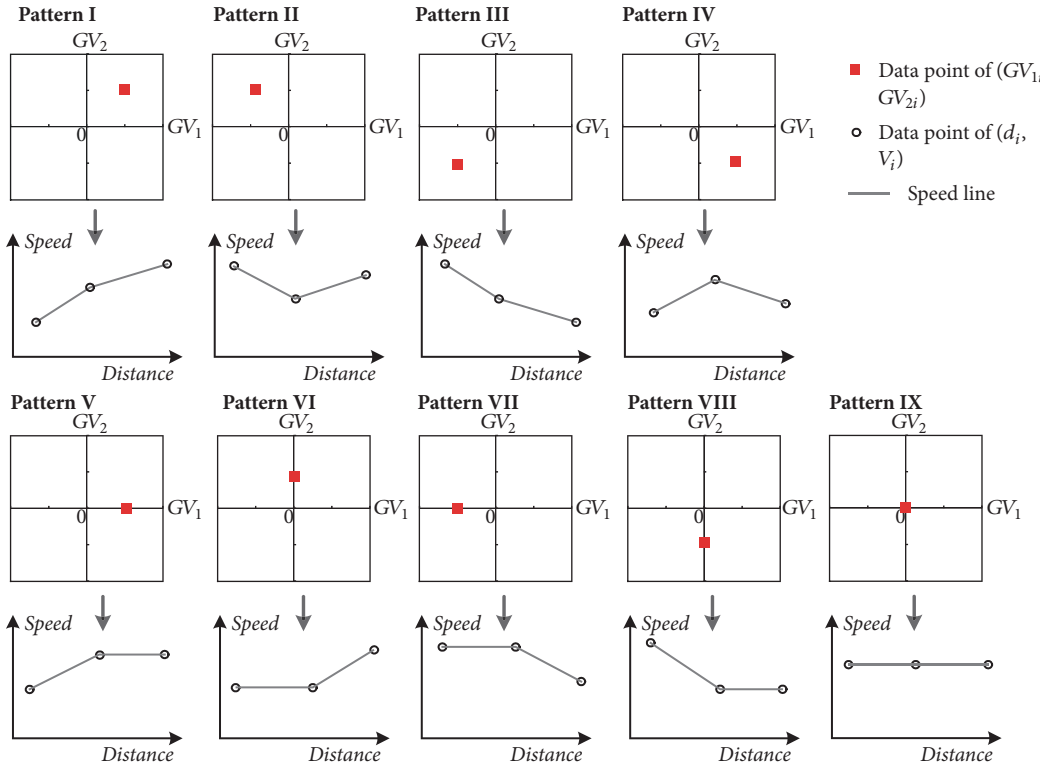

FIGURE 13: Identifying the speed pattern on helical ramp by using the position of an arbitrary data point (GV_{1i}, GV_{2i}) in GV_1 —GV_2 coordinate.

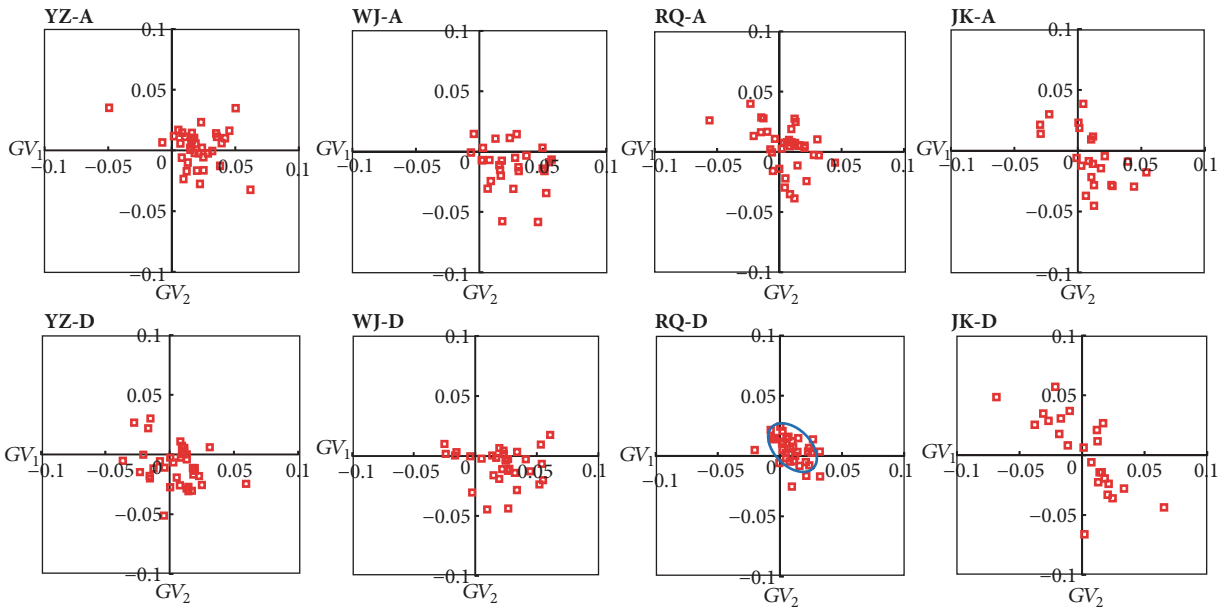

FIGURE 14: Data point (GV_{1i}, GV_{2i}) of four ascending helical ramps and four descending ramps shown in GV_1 —GV_2 coordinate, where YZ-A and YZ-D denote the ascending and descending ramp of Fuling Yangtze River Bridge, respectively; WJ-A and WJ-D denote the ascending and descending ramp of Fuling Wujiang Bridge; RQ-A and RQ-D denote the ascending and descending ramp of Rongqiao Helix Bridge; and JK-A and JK-D denote the ascending and descending lane of Jinkai ring bridge.

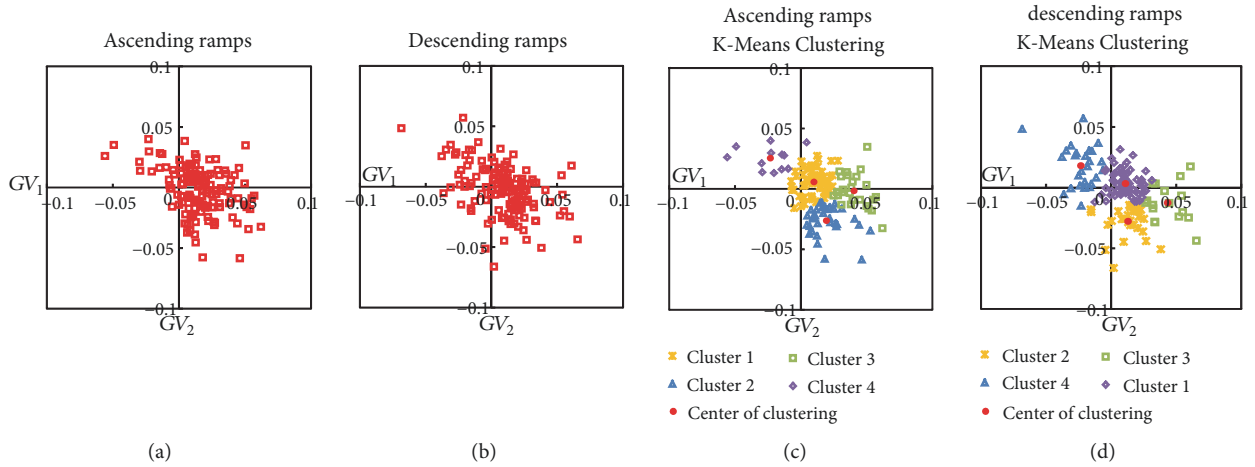

FIGURE 15: Scatter plot containing the points of (GV_{1i}, GV_{2i}) of four ascending/descending ramps. (a) Scatter plot of ascending ramps; (b) scatter plot of descending ramps; (c) four clusters for ascending ramps; (d) four clusters for descending ramps.

and V are dominant speed modes, while, for WJ' descending ramp, dominant speed patterns are IV, V, and VII.

Data points of RQ bridge and JK bridge have similar distribution characteristic; however, for RQ bridge the points' distribution is more concentrated, especially on RQ's descending lanes, which indicates that a convergent driving behavior occurs on this helical bridge.

Data points of all four ascending ramps were put together and displayed in one GV_1 —GV_2 coordinate, as shown in Figure 15(a); and Figure 15(b) for descending ramps was then obtained using the same method. In Figure 15(a) the number of data points located in the first to fourth quadrant is {N_1 = 53 (39%), N_2 = 65 (47.8%), N_3 = 14 (10.3%), N_4 = 4 (2.9%)}, while in Figure 15(b) this set of numbers is {N_1 = 39 (28.3%), N_2 = 62 (44.9%), N_3 = 24 (17.4), N_4 = 13 (9.4%)}. Therefore, pattern IV is dominant pattern for both ascending and descending ramps, followed by pattern I, and pattern III occupied the lowest share in the total. Figures 15(c) and 15(d) show four clustering results obtained by K-means arithmetic; the center of clustering distributes the quadrants except the third quadrant. Table 2 lists the coordinate values of the center of clustering for ascending/descending ramps and sample size of points divided into each cluster.

Table 2: Center of clustering for ascending/descending ramps.

	Ascending ramps				Descending ramps			
	Cluster 1	Cluster 2	Cluster 3	Cluster 4	Cluster 1	Cluster 2	Cluster 3	Cluster 4
Value of clustering center	(0.01, 0.0058)	(0.020,-0.0262)	(0.04,-0.00154)	(-0.023, 0.0255)	(0.01108, 0.00347)	(0.0131,-0.02772)	(0.0435, -0.01247)	(-0.0232, 0.0181)
sample size of each cluster	64	34	27	12	65	30	17	36

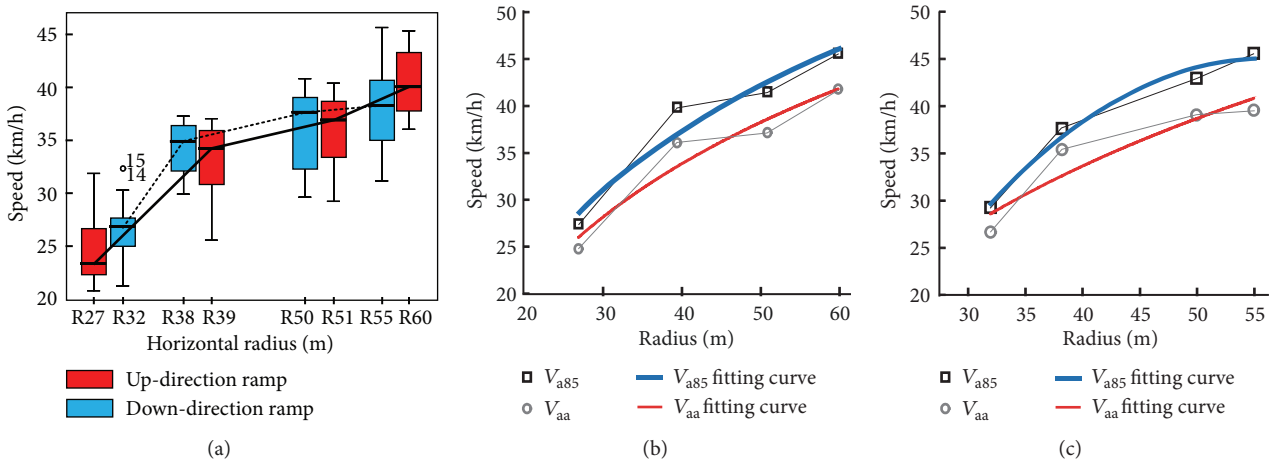

Figure 16: (a) Box plots of speed versus ramp radius; eigenvalue of driving speed and horizontal radius of (b) ascending ramp and (c) descending ramp.

Table 3: Regression model coefficients and the goodness of fit.

Object	b_1	b_2	R^2
Ascending ramp V_{a85}	21.803	-43.175	0.940
Ascending ramp V_{aa}	20.496	-41.87	0.906
Descending ramp V_{a85}	28.494	-68.198	0.962
Descending ramp V_{aa}	22.593	-49.712	0.876

6. Correlation between Speed and Ramp Radius

The box plot of the average speed on a helical ramp (the average value of a speed curve within Stage II in Figure 5 and Stage III in Figure 8), V_{ai}, was obtained using SPSS19.0, as shown in Figure 16(a). It is obvious from the figure that there is a correlation between the driving speed and horizontal radius of the helical ramp, regardless of whether it is an ascending or descending ramp; that is, the larger the radius, the higher the driving speed. The 85th percentile of V_{ai}, i.e., V_{a85}, for each helical ramp was extracted, and a broken line graph of V_{a85} changing over ramp radius was plotted, as shown in Figures 16(b) and 16(c), in addition to the quadric mean V_{aa}. From the figure, we can see a strong correlation between V_{a85} (or V_{aa}) and ramp radius. Using the least squares analysis, the regression formula for the data points in the graphs can be determined. Among various typical mathematical functions, logarithmic function has a higher goodness of fit and a simpler form, and it is expressed as follows:

$$f(x) = b_1 \cdot \ln(x) + b_2, \quad (4)$$

where x is the independent variable, namely, the horizontal radius of the centerline (m) of the bridge deck (box girder) where the traffic lane is located, and $f(x)$ is the function of the dependent variables V_{a85} or V_{aa}. The values of the regression model coefficients, b_1 and b_2, and the goodness of fit, R^2, are presented in Table 3.

7. Discussion

Based on the speed behavior of various participants measured in this study (speed profiles shown in Figures 5 and 8), we conclude that the design speed of the helical ramp of the Yangtze River Bridge is not appropriate, and the alignment elements are inconsistent with its design standard. This leads to a serious deviation between the actual driving behavior and design expectations. Therefore, the ramp radius, shoulder width, and other geometric features used in the design process should not significantly exceed the normal values recommended in the guideline; otherwise, the design speed should be increased to correspond to the design criteria of ramp geometry.

After the interchange construction is completed and opened to traffic, a proper speed limit for the ramp should be determined through an adequate field investigation and verification, rather than simply using the design speed of the ramp as the speed limit. A too low speed limit reduces the traffic capacity and the operational efficiency in ramp areas where there are no valid safety concerns. According to Figure 16, apart from R60 (ascending ramp of Rongqiao Helix Bridge), the 75th percentiles V_{ai}, V_{a75}, for other seven ramps, are less than 40 km/h. In addition, except for Jinkai Ring Bridge, the 85th percentile V_{ai}, V_{a85}, for the ramps at the other three sites, ranges from 40 to 45 km/h for the ascending path and 38 to 45 km/h for the descending path. Therefore, for one-way helical ramps and bridges with design speeds below 40 km/h, speed limit for passenger cars should be set at 40 km/h, i.e., the roundness of V_{a85} taking tens as unit. Moreover, because it is common for the drivers to decelerate in the traffic merge area (the end of the ramp), there is a high rear-end collision risk in that area when the deceleration amplitudes of the preceding and following vehicles are inconsistent. This fact also requires the attention of the designers and administrators.

For descending ramps, drivers experience an obvious deceleration when entering a helical ramp, and deceleration length and its distribution of WJ' ramp and RQ' ramp are

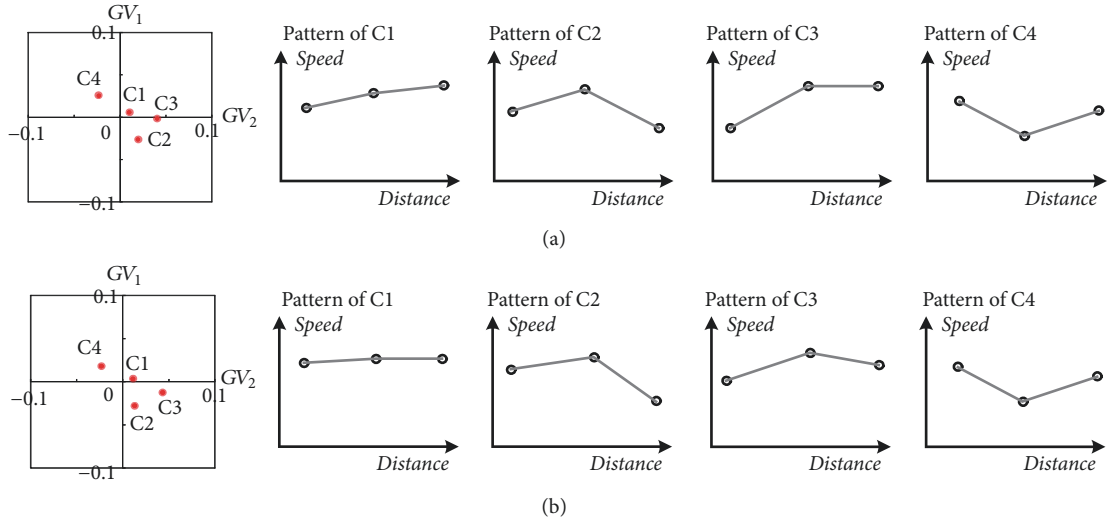

Figure 17: Speed patterns correspond to four clustering center. (a) Ascending ramp; (b) descending ramp.

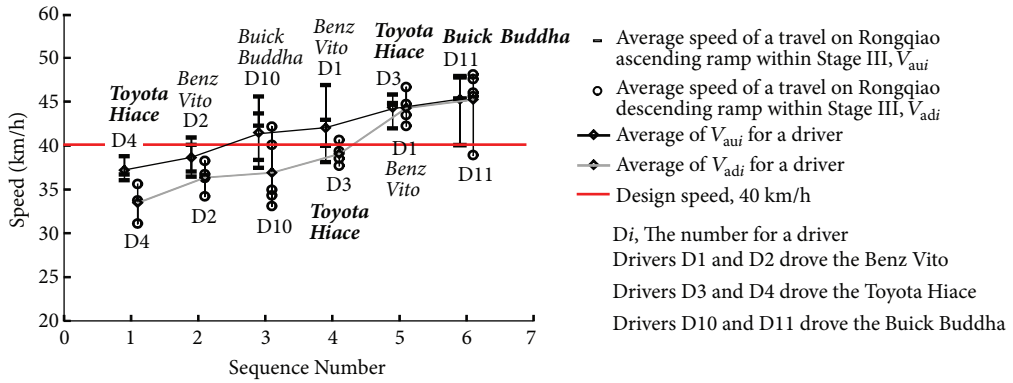

Figure 18: Average speed of different types of vehicles on Rongqiao Helical Bridge.

present in Section 4.2.2. The deceleration length of YZ' ramp was analyzed qualitatively, instead of getting a statistical distribution, because there are three curves between the tangent and the helix (see Figure 9); i.e., the helix is not directly connected to the tangent (mainline).

One of the main aims of this work is to get the speed pattern for helical ramps, a method of "location in four-quadrant of speed gradient (GV_{1i}, GV_{2i})" was designed to determine the speed patterns, and this method has an explicit physics meaning to explain the change in speed. In addition, four clusters by K-means algorithm are present in Figures 15(c) and 15(d); according to the location of four clustering centers in GV_1 —GV_2 coordinate, we can draw the four typical speed patterns, as shown in Figure 17.

The content of this study is a part of investigative work on the "identification and control of dangerous driving patterns on complex interchanges based on reverse deconstruction of multi-parameters (NSFC 51678099)," conducted by us. In the early stages of the driving experiments, we carried out driving tests on interchanges located in an urban area of Chongqing. While collecting the naturalistic data on the Rongqiao Helix Bridge, we became aware of the peculiarities of this type of ramp. Consequently, we searched for other examples of such interchanges within the jurisdiction of Chongqing and found Yangtze River Bridge and Wujiang Bridge in Fuling, a district of Chongqing. While conducting the driving tests in Fuling for the second time, we found another conspicuous object, the Jinkai Ring Bridge. Therefore, the number of participants for each experimental site was different because of the difference in the experiment period. And the sample of participants of all experimental sites is relatively small, which may reduce the statistical significance and result in a limitation of this study.

Another limitation of this paper is the two different types of vehicles adopted in the driving test, three MPVs and one minivan. Minivan (Toyota Hiace) has a higher center of gravity than the other three vehicles, which can result in a larger rolling moment that acted on the vehicle body and may influence the driving behavior. To figure out whether the effect exists, the average speeds within Stage III on Rongqiao Helical Bridge (Toyota Hiace was used on this site), V_{au} and V_{ad}, were calculated for each travel. And V_{aui} and V_{adi} for each participant were averaged again ($i = 1, 2. . . . . ., N$, N is number of rounds a driver's trip on the helical bridge), and then the quadric mean speed was obtained, as shown in Figure 18.

Next, we sequenced the quadric mean speed in an ascending order and then obtained two polylines for up- and down-direction travel. In Figure 18 driver D4 drove Toyota Hiace at the lowest speed, while driver D3 of the same vehicle steered at the second-highest speed. From Figure 18 we are not able to see a correlation between vehicle type and average driving speed, and maybe the driving style and personality of drivers are the dominant factors for the difference in driving speed. And this issue will be analyzed and discussed in our future work.

8. Conclusions

In this study, we conducted field driving tests and obtained the operating parameters of vehicles traveling on helical ramps under natural driving conditions. Based on the analysis of the naturalistic data of driving speed obtained from the participants, speed characteristics and speed patterns on helical ramps were determined, as well as factors affecting speed amplitudes and fluctuations. The findings in this study can provide basic data referencing and scientific evidence to essentially improve the safety level of helical ramps in the practice of design and operation stage. The main findings of our research are as follows:

(1) When a helical ramp merged with the main route, the driver would observe the traffic on the mainline and make a judgment to adjust his/her speed. Therefore, obvious deceleration behavior exhibited by the driver was observed before the physical gore, and this was common to all participants. When drivers entered a helical ramp from a tangent, they generally decelerated, and this deceleration behavior would last for a distance equal to approximately 33–40% of the circumference of the ramp.

(2) Speed along ascending ramps shows an overall stable or a slightly rising trend, and the continuously increasing elevation in ascending ramp did not cause a remarkable speed reduction for passenger car, while speed along descending ramps, except YZ' ramp, represents an overall stable trend, and the continuously decreasing elevation along the distance did not result in an obvious increase in the traveling speed.

(3) For one-lane helical ramps, the lower the design speed, the larger the discrepancy between the measured speed and design speed. Moreover, based on the distribution of the measured speed, 20 km/h should not be recommended as the design speed for helical ramps, and the consistency between the design speed and the alignment elements value of the ramp should be increased. In addition, for ramps with design speeds no larger than 40 km/h, the speed limit should be set to 40 km/h.

(4) We designed a method of "location in four-quadrant of speed gradient (GV_{1i}, GV_{2i})" to determine the speed patterns for individuals; this method has an explicit physics meaning to explain the change in speed. Moreover, four clusters were obtained by clustering the data points of (GV_{1i}, GV_{2i}) using K-means algorithm, and four typical speed patterns were thus determined.

(5) There is a high correlation between the driving speed and the ramp radius. The 85th percentile speed and the average speed increase with the increase in the ramp radius, and predicting models were developed.

In this work, we mainly analyzed the speed characteristics on helical ramps. Other key factors, such as lateral acceleration, lane occupancy, and steering/pedal input, will be described in another article. Moreover, during the natural driving test, we collected the electrocardiographic (ECG) signals of the drivers and passengers. In our future work, we will analyze the distribution and variation characteristics of ECG signals within helical ramps to obtain the mental workload of drivers and its influence on the driving behavior.

Data Availability

The data used to support the findings of this study are available from the corresponding author upon request.

Conflicts of Interest

The authors declare that there are no conflicts of interest regarding the publication of this article.

Acknowledgments

This research was supported by the National Natural Science Foundation of China (Grant No. 51678099) and by Applied Basic Research Program of Ministry of Transport of China (Grant No. 2015319814050).

References

[1] Y.-P. Zhao, S.-W. Yang, H.-J. Wu, Y.-F. Zhao, and B.-H. Pan, "Helix line development's minimum radius of horizontal curve in freeway tunnel," *Journal of Chang'an University*, vol. 27, no. 6, pp. 72–75, 2007.

[2] G. Yang, H. Xu, Z. Tian, and Z. Wang, "Vehicle speed and acceleration profile study for metered on-ramps in california," *Journal of Transportation Engineering*, vol. 142, no. 2, pp. 1–13, 2016.

[3] W. Zhang, "Discussion on new kind of T-shaped interchange design," *Transportation Science and Technology*, vol. no.5, pp. 145–147, 2014.

[4] Y. P. Lai, C. Yang, and G. L. Ren, "Design of spiral ramp bridge of the second FulingWujiang River Bridge," *Bridge Construction*, no. 1, pp. 47–50, 2007.

[5] S. Ivorra, D. Foti, D. Bru, and F. J. Baeza, "Dynamic behavior of a pedestrian bridge in alicante, Spain," *Journal of Performance of Constructed Facilities*, vol. 29, no. 5, pp. 1–10, 2015.

[6] W. Wang, "Foundation treatment for double-deck spiral bridge on Chongqing Rongqiao Avenue," *Building Construction*, vol. 32, no. 8, pp. 864-865, 2010.

[7] Z. Y. Zhang, X. Y. Hao, W. B. Wu, and D. Wang, "The running speed prediction model of interchange ramp," *Journal of Transportation Systems Engineering and Information Technology*, vol. 15, no. 1, pp. 93–99, 2015.

[8] C. Zhang, X. M. Yan, X. W. Li, B. H. Pan, H. J. Wang, and X. N. Ma, "Operating speed model of passenger car at single-lane exit of interchange," *China Journal of Highway and Transport*, vol. 30, no. 6, pp. 279–286, 2017.

[9] H. J. Wang and S. W. Yang, "Research of length of deceleration lane at expressway interchange," *Journal of Highway and Transportation Research and Development*, vol. 32, no. 3, pp. 124–128, 2015.

[10] Z. Guo, H. Wan, Y. Zhao, H. Wang, and Z. Li, "Driving simulation study on speed-change lanes of the multi-lane freeway interchange," *Procedia: Social and Behavioral Sciences*, vol. 96, pp. 60–69, 2013.

[11] R. H. Wang, J. B. Hu, and X. Q. Zhang, "Analysis of the driver's behavior characteristics in low volume freeway interchange," *Mathematical Problems in Engineering*, vol. 2016, Article ID 2679516, 9 pages, 2016.

[12] A. Polus, M. Livneh, and J. Factor, "Vehicle flow characteristics on acceleration lanes," *Journal of Transportation Engineering*, vol. 111, no. 6, pp. 595–606, 1985.

[13] M. Livneh, A. Polus, and J. Factor, "Vehicle behavior on deceleration lanes," *Journal of Transportation Engineering*, vol. 114, no. 6, pp. 706–717, 1988.

[14] M. A. Ahammed, Y. Hassan, and T. A. Sayed, "Modeling driver behavior and safety on freeway merging areas," *Journal of Transportation Engineering*, vol. 134, no. 9, pp. 370–377, 2008.

[15] K. Fitzpatrick, S. T. Chrysler, and M. Brewer, "Deceleration lengths for exit terminals," *Journal of Transportation Engineering*, vol. 138, no. 6, pp. 768–775, 2012.

[16] B. Zirkel, S. Park, J. McFadden, M. Angelastro, and L. McCarthy, "Analysis of sight distance, crash rate, and operating speed relationships for low-volume single-lane roundabouts in the united states," *Journal of Transportation Engineering*, vol. 139, no. 6, pp. 565–573, 2013.

[17] P. Perco, A. Marchionna, and N. Falconetti, "Prediction of the operating speed profile approaching and departing intersections," *Journal of Transportation Engineering*, vol. 138, no. 12, pp. 1476–1483, 2012.

[18] B. Yang, "Urban interchange in chongqing-grade separation project with mountainous characteristic," *Urban Roads Bridges and Flood Control*, no. 9, pp. 46–49, 2016.

[19] G. Li and L. Sun, "Characterizing heterogeneity in drivers' merging maneuvers using two-step cluster analysis," *Journal of Advanced Transportation*, vol. 2018, Article ID 5604375, 15 pages, 2018.

[20] N. Lyu, Y. Cao, C. Wu, J. Xu, and L. Xie, "The effect of gender, occupation and experience on behavior while driving on a freeway deceleration lane based on field operational test data," *Accident Analysis & Prevention*, vol. 121, pp. 82–93, 2018.

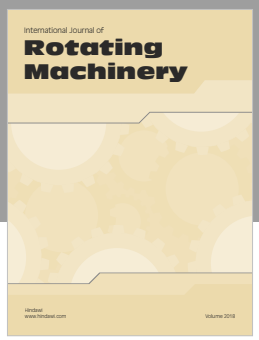

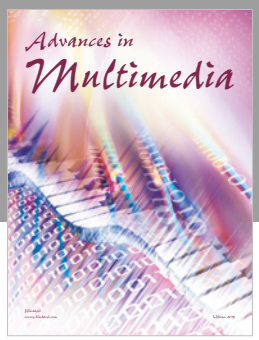

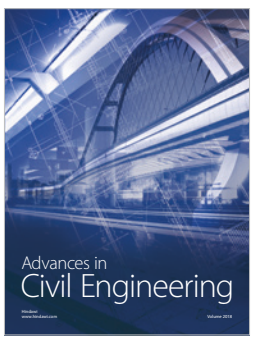

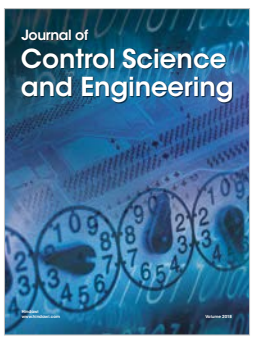

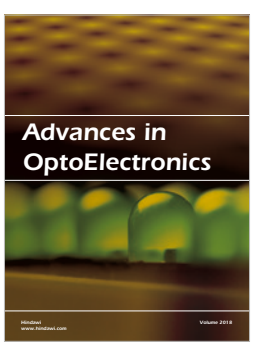

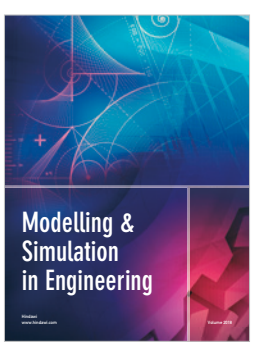

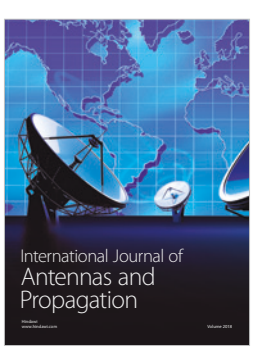

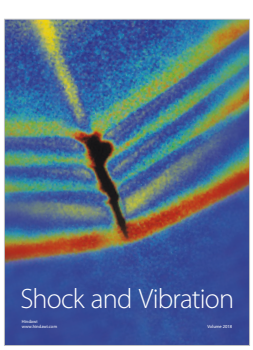

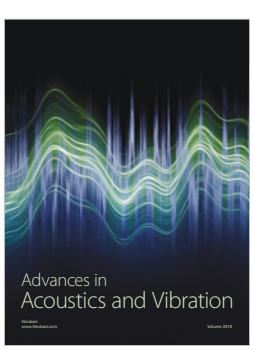

Hindawi

Submit your manuscripts at
www.hindawi.com